PCCP

PAPER

View Article Online
View Journal | View Issue

Cite this: *Phys. Chem. Chem. Phys.*, 2016, **18**, 5159

# Spontaneous polarization of solid CO on water ices and some astrophysical implications

Alexander Rosu-Finsen,[a] Jérôme Lasne,[ab] Andrew Cassidy,[c] Martin R. S. McCoustra[a] and David Field*[c]

Received 17th November 2015,
Accepted 17th December 2015

DOI: 10.1039/c5cp07049j

www.rsc.org/pccp



Reflection absorption infrared spectroscopy (RAIRS) is used to show that when 20 monolayer (ML) films of solid CO are laid down on solid water substrates at 20 to 24 K, the films polarize spontaneously. CO films were prepared on three types of water ice: porous amorphous solid water (CO-$p_{ASW}$), crystalline water (CO-CSW) and compact amorphous solid water (CO-$c_{ASW}$) with corresponding fields of $3.76 \pm 0.15 \times 10^7$ V m$^{-1}$ for CO-$p_{ASW}$, $2.87 \pm 0.15 \times 10^7$ V m$^{-1}$ for CO-CSW and $1.98 \pm 0.15 \times 10^7$ V m$^{-1}$ for CO-$c_{ASW}$. For comparison, CO laid down on $SiO_2$ yields $3.8 \pm 0.15 \times 10^7$ V m$^{-1}$. Our results are of relevance to an understanding of the chemistry and physics of dense star-forming regions in the interstellar medium, in which dust particles become coated with solid CO on a layer of $c_{ASW}$. The polarization charge which accumulates on the CO surface acts as a catalyst for the removal of electrons and ions from the medium and may account for the low degree of ionization observed in these regions, a feature which is an important factor for the rate of star formation.

## 1. Introduction

Previous work has shown that when a dipolar molecular gas is condensed onto a cold substrate, a solid film may be formed which spontaneously exhibits a static electric field,[1–9] the strength of which may exceed $10^8$ V m$^{-1}$. Such solid films are referred to as spontelectric, an elision of 'spontaneously electrical'. Spontelectric materials discovered to date all possess a permanent dipole moment and range over CO, hydrocarbons, halocarbons, alcohols, organic formates, benzene derivatives and such simple inorganics as nitrous oxide. Fields are created through dipole orientation, as numerous studies have now conclusively demonstrated. Spontelectrics represent a new structural and electrical phase of solids. The spontelectric phase may be experimentally characterised by direct measurement of potentials on the surface of films of material or, as has been shown very recently, by reflection–absorption infrared spectroscopy (RAIRS).[8,9] This is the technique which is used in the present work.

The principle of the RAIRS experiment is as follows. The spontelectric field in the film creates a Stark shift[10] in vibrational frequencies measured in RAIRS. Since the strength of the spontelectric field depends on the temperature of deposition of the film of material, there is a corresponding temperature dependence of the vibrational frequencies measured using RAIRS. For example the electric field in $N_2O$ decreases by a factor of 2.3 between deposition temperatures of 48 K and 62 K.[1] There is an accompanying Stark shift in vibrational energy levels, involved in the $\nu$NN stretch, of 1.2 cm$^{-1}$. Such measurements of the shift in characteristic vibrational frequencies, as a function of deposition temperature, are diagnostic of the spontelectric effect. As discussed in detail in ref. 8 and 9, volume changes of the material contribute negligibly to the temperature dependence of vibrational frequencies. Observed Stark shifts may then be used to characterise the spontelectric field in the material. The proof of principle of this method was provided by a RAIRS study of $N_2O$ films[8] and the technique has been used to study CO ices,[9] both deposited directly on a $SiO_2$ surface. Here we extend these studies to include CO deposited on various forms of water ice, composed of crystalline solid water (CSW), compact amorphous solid water ($c_{ASW}$) and porous amorphous solid water ($p_{ASW}$).

The reasons for conducting the present study are twofold. First, we seek further to exploit the readily accessible technique of RAIRS as a means of performing new detections of the spontelectric effect in films, in this case of heterolayered films.[11]

[a] *Institute of Chemical Sciences, Heriot-Watt University, Riccarton, EH14 4AS Edinburgh, UK*
[b] *Laboratoire Interuniversitaire des Systèmes Atmosphériques (LISA), CNRS UMR 7583, Université Paris-Est Créteil, Université Paris Diderot, Faculté des Sciences et Technologie, 61 avenue du Général de Gaulle, 94010 Créteil Cedex, France*
[c] *ISA, Department of Physics and Astronomy, Aarhus University, DK-8000 Aarhus C, Denmark. E-mail: dfield@phys.au.dk*

Second, and on a quite different tack, there are significant astrophysical applications, in the field of star formation, associated with solid CO on water ice. It is known through observation of these so-called pre-stellar cores, that CO is heavily depleted from the gas phase through condensation on interstellar grains,[12,13] already coated with a water ice mantle. The data which we present here show that such grains, with a CO layer on top of a water ice substrate, are likely to harbour several polarization charges. Following results in ref. 14, we expect these polarization charges to be positive at the CO-vacuum interface. This could contribute to the low values of the observed degree of ionization in such prestellar cores.[15,16] The present report therefore supplies useful information for modelling of these noteworthy regions in the interstellar medium, which are on the verge of gravitational collapse to form a star.

As described in the experimental Section 2, spontelectric films are studied using RAIRS with a grazing infrared beam. Thus the incident electric field of the beam has components both parallel and perpendicular to the film normal. Relative to the incident beam wavelength, the film can be considered infinite in the plane of the film and only transverse optical (TO) phonons can be excited in this plane. If however the thickness of the film is comparable to the wavelength of the incident beam, the boundary conditions allow for the excitation of longitudinal optical (LO) phonons along the normal axis. This is known as the Berreman effect,[17] and has been studied extensively in non-ionic films.[18–20] Longitudinal phonons resonate at higher frequencies, because of the induced field associated with longitudinal waves passing through a medium composed of dipolar species. Thus when an incident beam interrogates a thin film at a suitably oblique angle, any vibrational mode has two components and is subject to so-called LO–TO splitting.

Henceforth $\nu_L$ and $\nu_T$ represent the frequencies for LO and TO phonons respectively and $\Delta\nu = \nu_L - \nu_T$ represents the value of the splitting. The force fields giving rise to $\nu_L$ and $\nu_T$ are modified by the vibrational Stark effect, through the presence of the spontelectric field associated with the film of solid CO. We have shown in detail in ref. 9 how we may relate the resulting modification of LO–TO splitting, and its temperature dependence, to the presence of a static spontelectric field, oriented along the surface normal of the film. This is summarized in the present work in Section 3. We demonstrate how measurements of $\nu_L$ and $\nu_T$, as a function of deposition temperature, may then lead to a characterization of the spontelectric field in CO on CSW, $c_{ASW}$ and $p_{ASW}$. For simplicity, we refer throughout to the observed splitting in RAIR spectra as LO–TO splitting. At the same time, we recognize that the absolute value of the splitting arises through a combination of the intrinsically different vibrational frequencies associated with LO and TO modes and, at the level of approximation adopted here, an independent contribution due to the vibrational Stark effect. We find, for example, that at a deposition temperature of 20 K, the Stark effect contributes 54% of the total measured splitting of 4.59 $cm^{-1}$ for CO deposited on CSW (CO-CSW). Moreover, the observed deposition temperature dependence of LO–TO splitting, in this case of 4.59 to 4.18 $cm^{-1}$ between temperatures of 20 K and 24 K, may be attributed wholly to the dependence of the spontelectric field on the film deposition temperature.

# 2. Experimental method and results

## 2.1. The experimental method

RAIRS experiments were performed using an ultrahigh vacuum system, described in detail elsewhere.[21,22] The substrate, an oxygen-free high conductivity copper block coated with 300 nm of amorphous silica, is mounted on the end of a closed-cycle helium cryostat, reaching a base temperature of 18 K, measured with a KP-type thermocouple connected to an IJ-6 temperature controller (IJ Instruments). The central chamber is equipped with a line-of-sight quadrupole mass spectrometer (QMS, Hiden Analytical) and a Fourier-transform infrared spectrometer (Varian 670-IR) used in reflection–absorption mode, at a grazing incidence of 75° with respect to the normal to the substrate. After reflection from the sample, the infrared beam is focused into a liquid nitrogen cooled HgCdTe detector. The RAIR spectra presented here result from co-addition of 512 spectra recorded at a resolution of 0.1 $cm^{-1}$.

The layered films, consisting of 20 ML of CO on 50 ML of water, are deposited by background dosing of $H_2O$ (Fluka, purity 99.9%) and CO gas (BOC, purity 99.9%) onto the substrate at a rate of 0.04 ML $s^{-1}$ and 0.05 ML $s^{-1}$, respectively. Deposition of $H_2O$ at a substrate temperature of 18 K, 110 K and 140 K ensured respectively, $p_{ASW}$, $c_{ASW}$ and CSW.[23–26] The substrate was cooled and CO was dosed at 20 K, 22 K or 24 K, save for CO-$c_{ASW}$ in which the lowest temperature of dosing was 21 K. Thicknesses of $H_2O$ and CO films in monolayers (ML) were determined (±20%) through temperature-programmed desorption (TPD) experiments, performed by applying a heating ramp of 0.2 K $s^{-1}$ for CO desorption and 0.1 K $s^{-1}$ for $H_2O$ desorption from the base temperature of 18 or 20 K. The desorbed species were detected using the QMS.

## 2.2. Results

The RAIR spectra of the $\nu$CO band of 20 ML CO deposited as CO-CSW, CO-$p_{ASW}$ and CO-$c_{ASW}$ at various temperatures are presented in Fig. 1a–c, respectively. The insets in Fig. 1 show the change in the appearance of the OH stretching band of $H_2O$ in CSW, p-ASW and c-ASW.

The CO band exhibits LO–TO splitting, with the LO mode for example at 2142.96 $cm^{-1}$ and the TO mode at 2138.08 $cm^{-1}$ at 20 K for CO-$p_{ASW}$. The LO mode red-shifts while the TO mode blue-shifts as the deposition temperature is increased from 20 K to 24 K, as Fig. 1 shows. Data for RAIRS spectra of CO at deposition temperatures above 24 K are not presented, since desorption from the different water substrates occurs at these higher temperatures,[27] unlike CO deposited directly on the $SiO_2$ surface.[9,28] Just as for CO films deposited directly on $SiO_2$ and annealed, annealing CO films deposited on the $H_2O$ layers does

 

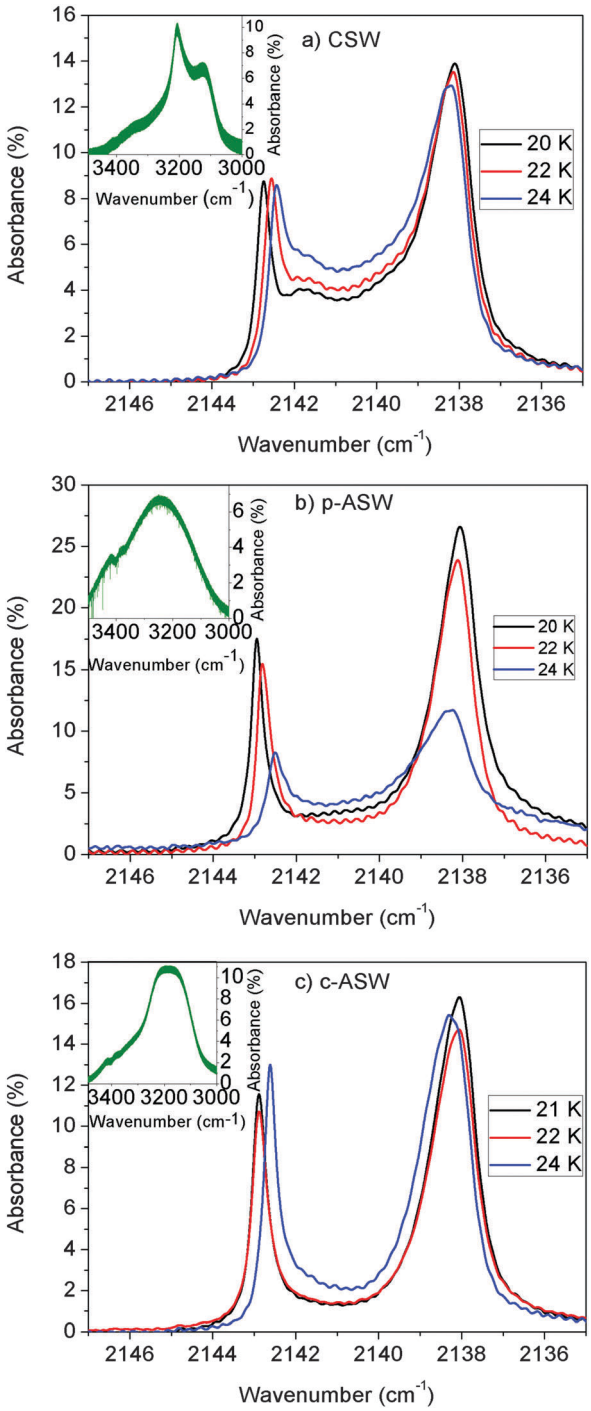


Fig. 1 RAIR spectra collected after CO has been deposited at 20 or 21 (black), 22 (red) and 24 (blue) K on CSW (a), $p_{ASW}$ (b) and $c_{ASW}$ (c). The insets in each graph show the OH stretch for the water substrate beneath the CO layer. In each case a contraction in the LO–TO splitting of the CO stretching mode is seen as the deposition temperature increases.

not produce detectable shifts in the LO and TO modes. Desorption of CO was not observed at the temperatures used for this work as confirmed by TPD experiments[27] and a $\nu$CO band intensity was found to be constant within ~6% during the annealing experiment from a base temperature of 20 K to 24 K.

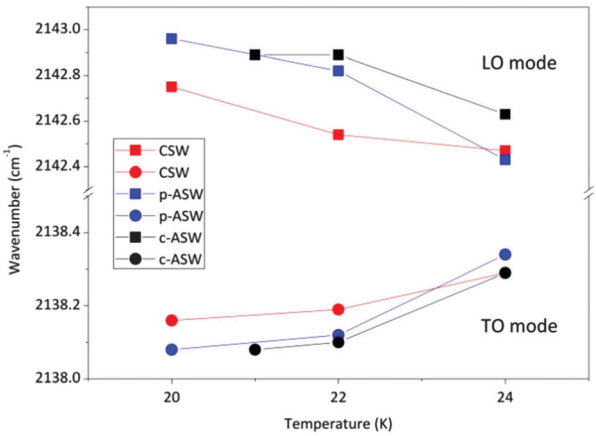


Fig. 2 Peak positions of the $\nu$CO band as plotted with deposition temperature. The square symbols represent the LO mode, while the round symbols represent the TO mode of CO on $p_{ASW}$ (blue), $c_{ASW}$ (black) and CSW (red). The lines are a guide to the eye.

The LO and TO modes of the $\nu$CO band of CO films on the different $H_2O$ substrates were fitted with Gaussian functions using the Igor Pro software, following a procedure described in ref. 9. This gave an accuracy of $\pm 0.01$ cm$^{-1}$ and $\pm 0.02$ cm$^{-1}$ for the location of the peak maximum of the LO and TO modes, respectively. Fig. 2 has been constructed from this analysis showing the peak positions of the LO and TO modes of CO-$p_{ASW}$ (blue), CO-$c_{ASW}$ (black) and CO-CSW (red) with respect to deposition temperature. The red-shift of the LO band and the blue shift of the TO band, with increasing deposition temperatures, may clearly be seen in Fig. 2.

The continuum between the LO and TO peaks is created through inhomogeneous broadening. Greater broadening indicates a larger range of molecular environments and here we briefly consider the connection with the degree of dipole orientation with reference to the underlying ice structure. Measurement of the broadening was performed from the intensity of the RAIR

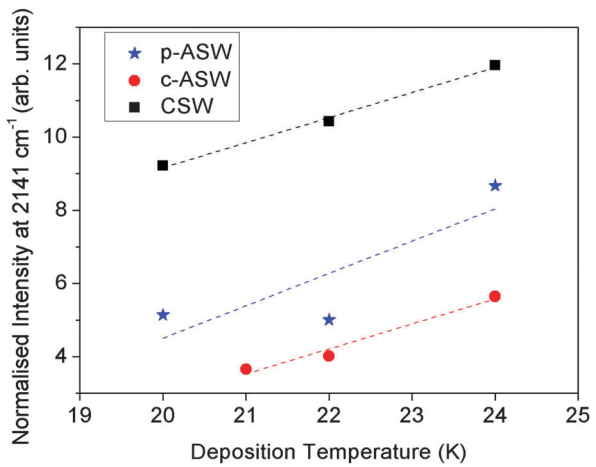


Fig. 3 Intensity measured at 2141 cm$^{-1}$ in the RAIR spectra normalized by the total area of the $\nu$CO band for each substrate, as a function of deposition temperature. The dotted line results from a linear fit of the data and is only presented here to guide the eye.

spectra at 2141 $cm^{-1}$, essentially the average of the LO and TO modes, and normalising this with the integrated area of the entire $\nu$CO band. This normalisation allows the inhomogeneous broadening to be compared between different experiments at different temperatures, on any one material. Fig. 3 shows this measurement for the CO film on the various $H_2O$ underlayers. Insofar as inhomogeneous broadening, for any one of the three cases, is a measure of the range of environments in which any CO species finds itself, the greater the inhomogeneous broadening the less the dipole orientation. Results in Fig. 3 are therefore consistent with the expected behaviour of a spontelectric material, and may be understood to show the expected drop in dipole orientation with increasing deposition temperature.[1]

Fig. 3 also shows that CO-CSW exhibits the highest degree of inhomogeneity, with CO-$c_{ASW}$ and CO-$p_{ASW}$ indicating a lesser extent. The greater inhomogeneity exhibited for CO-$p_{ASW}$, compared to CO-$c_{ASW}$, may be due to the pores in $p_{ASW}$ leading to a range of binding sites for CO not present in $c_{ASW}$. The high value for CO-CSW cannot be readily accounted for, save to state that in the conventional view this ice would be $I_c$ ice and that such ice is imperfect in structure, perhaps providing numerous distinct binding sites for CO.[29]

# 3. Determination of the spontelectric fields in CO ices

Our object here is to determine the spontelectric fields and degrees of dipole orientation in CO-CSW, CO-$p_{ASW}$ and CO-$c_{ASW}$ ices, from the data in Section 2.2. This is carried out on similar lines to the data for CO-$SiO_2$ layers in ref. 9, where the method is described in detail. For ease of reference, Table 1 shows the definition of the various symbols used here.

## 3.1. Data in tabular form

The data shown in Fig. 1a–c are shown in tabular form in Tables 2–4 for CO-CSW, CO-$p_{ASW}$ and CO-$c_{ASW}$ respectively.

Table 1 Glossary of symbols used in Section 3

| Symbol | Description |
|---|---|
| Terms referring directly to experimental data | |
| $\nu_L$ | Longitudinal optical (LO) frequency |
| $\nu_T$ | Transverse optical (TO) frequency |
| $\Delta\nu$ | Measured LO–TO splitting |
| $\Delta\nu_S$ | Splitting due to the spontelectric Stark field |
| $\Delta\nu_B$ | Intrinsic splitting |
| $\xi$ | $\Delta\nu_S/\Delta\nu$ |
| Terms involved in modelling | |
| $\mu$ | Dipole moment of CO in the solid state |
| $\langle\mu_z\rangle/\mu$ | Degree of dipole orientation |
| $\Omega$ | Parameter related to the molecular volume of CO |
| $T$ | Temperature of deposition |
| $\zeta$ | Locking term parameter in eqn (2) |
| $E_S$ | Spontelectric field |
| $\langle E_{sym}\rangle$ | Symmetric field parameter |
| $\langle E_{asym}\rangle$ | Asymmetric field parameter = $(\langle\mu_z\rangle/\mu)/\varepsilon_0\Omega$ |

Table 2 RAIRS data for CO-CSW. Column 1: deposition temperature. Columns 2, 3: the frequency of the TO, LO vibrations. Column 4: the total LO–TO splitting. Column 5: the contribution of the spontelectric Stark effect to the total LO–TO splitting, based upon $\Delta\nu_B$ = 2.119 $cm^{-1}$ (see text). Column 6: the ratio of the Stark effect splitting to the total

| $T$/K | TO/$cm^{-1}$ ± 0.02 | LO/$cm^{-1}$ ± 0.01 | $\Delta\nu$/$cm^{-1}$ ± 0.03 | $\Delta\nu_S$/$cm^{-1}$ | $\xi = \Delta\nu_S/\Delta\nu$ |
|---|---|---|---|---|---|
| 20 | 2138.16 | 2142.75 | 4.59 | 2.471 | 0.538 |
| 22 | 2138.19 | 2142.54 | 4.35 | 2.231 | 0.513 |
| 24 | 2138.29 | 2142.47 | 4.18 | 2.061 | 0.493 |

Table 3 RAIRS data for CO-$p_{ASW}$. Column 1: deposition temperature. Columns 2,3: the frequency of the TO, LO vibrations. Column 4: the total LO–TO splitting. Column 5: the contribution of the spontelectric Stark effect to the total LO–TO splitting, based upon $\Delta\nu_B$ = 2.119 $cm^{-1}$ (see text). Column 6: the ratio of the Stark effect splitting to the total

| $T$/K | TO/$cm^{-1}$ ± 0.02 | LO/$cm^{-1}$ ± 0.01 | $\Delta\nu$/$cm^{-1}$ ± 0.03 | $\Delta\nu_S$/$cm^{-1}$ | $\xi = \Delta\nu_S/\Delta\nu$ |
|---|---|---|---|---|---|
| 20 | 2138.08 | 2142.96 | 4.88 | 2.761 | 0.566 |
| 22 | 2138.12 | 2142.82 | 4.70 | 2.581 | 0.549 |
| 24 | 2138.34 | 2142.43 | 4.09 | 1.971 | 0.482 |

Table 4 RAIRS data for CO-$c_{ASW}$. Column 1: deposition temperature. Columns 2,3: the frequency of the TO, LO vibrations. Column 4: the total LO–TO splitting. Column 5: the contribution of the spontelectric Stark effect to the total LO–TO splitting, based upon $\Delta\nu_B$ = 2.119 $cm^{-1}$ (see text). Column 6: the ratio of the Stark effect splitting to the total

| $T$/K | TO/$cm^{-1}$ ± 0.02 | LO/$cm^{-1}$ ± 0.01 | $\Delta\nu$/$cm^{-1}$ ± 0.03 | $\Delta\nu_S$/$cm^{-1}$ | $\xi = \Delta\nu_S/\Delta\nu$ |
|---|---|---|---|---|---|
| 21 | 2138.08 | 2142.89 | 4.81 | 2.891 | 0.559 |
| 22 | 2138.10 | 2142.89 | 4.79 | 2.671 | 0.558 |
| 24 | 2138.29 | 2142.63 | 4.34 | 2.221 | 0.512 |

The total splitting observed, $\Delta\nu$, is a sum of that part due to the spontelectric field, $\Delta\nu_S$, plus the intrinsic LO–TO splitting, $\Delta\nu_B$. If we plot the observed LO–TO splitting *versus* $T^{-1}$ and extrapolate to high $T$, as in ref. 9, we find for example for the CO-CSW data that $\Delta\nu_B$ = 2.119 $cm^{-1}$. This may be compared with the value of $\Delta\nu_B$ = 2.59 $cm^{-1}$ for CO–$SiO_2$. Numerical experiments show however that parameters derived for the spontelectric field are robust to a range of values of $\Delta\nu_B$. For example for CO deposited at 22 K on CSW ice, the spontelectric field is found to be 2.84 × $10^7$ V $m^{-1}$ using $\Delta\nu_B$ = 2.59 $cm^{-1}$ and 2.79 × $10^7$ V $m^{-1}$ using $\Delta\nu_B$ = 2.119 $cm^{-1}$, a variation in the field of <2%. This may be compared with an error resulting from random experimental uncertainties of ±5%.

The grounds for this lack of sensitivity, of the derived field to the absolute values of splitting, is that the derived spontelectric field is most influenced by the temperature dependence of $\Delta\nu_S$, rather than the absolute values. This is clear from the analysis presented in ref. 8 in sections 3.4.2, 3.4.3 and results shown in Table 2 of that paper. Moreover the intuitive notion that a greater spontelectric Stark field should lead to a proportionately larger spontelectric splitting does not hold, as we see below. In Tables 2–4, we have used

 

Table 5 Values of $\langle E_{sym}\rangle$, of the spontelectric field, $E_S$, and of the degree of dipole orientation for CO deposited on the three underlying substrates, crystalline solid water (CSW), porous amorphous solid water ($p_{ASW}$) and compact amorphous solid water ($c_{ASW}$) for deposition temperatures of 20, 22 and 24 K. Values shown are the upper branch solutions, as discussed in 3.3. Data are also shown for CO deposited on $SiO_2$, taken from ref. 9. Uncertainties given are random errors. Values are also quoted for both an intrinsic splitting, $\Delta\nu_B$, of 2.119 $cm^{-1}$ and of 2.59 $cm^{-1}$ (see text)

| | $\langle E_{sym}\rangle/10^7$ V $m^{-1}$ $\pm$ 0.1 $\times$ $10^7$ | $E_S/10^7$ V $m^{-1}$ $\pm$ 0.15 $\times$ $10^7$ | | | $\langle\mu_z\rangle/\mu \pm 0.0024$ | | | |
|---|---|---|---|---|---|---|---|---|
| | | 20 K | 22 K | 24 K | 20 K | 22 K | 24 K | $\Delta\nu_B/cm^{-1}$ |
| CSW | 3.74 | 2.89 | 2.84 | 2.77 | 0.0302 | 0.0247 | 0.0200 | 2.59 |
| | | 2.85 | 2.79 | 2.72 | 0.0291 | 0.0239 | 0.0193 | 2.119 |
| p-ASW | 4.68 | 3.73 | 3.65 | 3.72 | 0.0496 | 0.0401 | 0.0408 | 2.59 |
| | | 3.79 | 3.72 | 3.78 | 0.0516 | 0.0417 | 0.0424 | 2.119 |
| c-ASW | 3.16 | 1.99[a] | 1.83 | 1.89 | 0.0102[a] | 0.0072 | 0.00725 | 2.59 |
| | | 1.96[a] | 1.80 | 1.86 | 0.0097[a] | 0.0068 | 0.0069 | 2.119 |
| $SiO_2$[9] | 4.48 | 3.78 | 3.72 | 3.66 | 0.0645 | 0.0526 | 0.0434 | 2.59 |

[a] For data taken at 21 K deposition temperature.



$\Delta\nu_B$ = 2.119 $cm^{-1}$. We also present our conclusions, in Section 3.3, Table 5, for both $\Delta\nu_B$ = 2.119 $cm^{-1}$ and 2.59 $cm^{-1}$, to emphasise the insensitivity of the derived spontelectric field to our lack of accurate knowledge of $\Delta\nu_B$. Thus uncertainties in the derived spontelectric fields and the degrees of dipole orientation include the effect of possible systematic errors in $\Delta\nu_B$.

### 3.2. The model for the spontelectric effect

A detailed description of a model for the spontelectric effect may be found in ref. 1. This introduces the concept that constituent molecules in the film experience (i) a local symmetric field, $\langle E_{sym}\rangle(1+\zeta(\langle\mu_z\rangle/\mu)^2)$, where $\langle E_{sym}\rangle$ and $\zeta$ are derived from fitting to experimental data. Here $\langle\mu_z\rangle/\mu$, is the temperature dependent degree of dipole orientation, defined as the ratio of the average $z$-component of the dipole moment and the total dipole moment of the molecular species in the solid state. (ii) An asymmetrical field, the spontelectric field, $E_S$, given by $4\pi(\langle\mu_z\rangle/\mu)\mu/\Omega$, where $\Omega$, related to the molecular volume, may be treated as a parameter of the model.

The net field in the $z$-direction, normal to the plane of the film, is given by

$$E_z = \langle E_{sym}\rangle\left[1+\zeta\left(\frac{\langle\mu_z\rangle}{\mu}\right)^2\right] - E_S \qquad (1)$$

We note that the symmetrical part of the contribution to $E_z$ is related to the 'local field' at any molecular site, as defined in standard texts.[30]

Mean field theory gives an implicit expression for $\langle\mu_z\rangle/\mu$, yielding the familiar Langevin function for orientational interactions[30]

$$\frac{\langle\mu_z\rangle}{\mu} = \coth\left(\frac{E_z\mu}{T}\right) - \left(\frac{E_z\mu}{T}\right)^{-1} \qquad (2)$$

where $T$ is the deposition temperature of the layer of material. Note that atomic units (au) are used here, in which the Boltzmann constant is unity and $\varepsilon_0$ is $1/4\pi$.

Dipole moments in the solid state are reduced from those in the gas phase through depolarization according to:

$$\mu = \frac{\mu_0}{1+\alpha k/s^3} \qquad (3)$$

where $s$ is the average spacing between successive layers, $\alpha$ is the molecular polarizability for CO (13.159 au), $k$ = 11.034[31] and $\mu_0$ is the gas phase dipole moment, which for CO is 0.122 D. $s$ is estimated for CO from the diameter of isoelectronic $N_2$ to be 0.339 nm or 6.406 au. In the absence of any other data, $s$ is assumed to take on the same value for CO-$p_{ASW}$, CO-$c_{ASW}$ and CO-CSW.

### 3.3. Derivation of spontelectric fields in CO-CSW, CO-$p_{ASW}$ and CO-$c_{ASW}$

It was shown in ref. 8 and 9 that $(U_L - U_T)/U_T \sim \Delta\nu/\nu_T$, where $U_T$ is the energy associated with the TO vibration and $U_L$ with the LO vibration. Additionally, $U_L - U_T \propto$ the spontelectric field times the degree of dipole orientation and $U_T \propto$ to the symmetric part of the field times $\Delta\nu/\Delta\nu_S$. That is, $U_T \propto \xi^{-1}\langle E_{sym}\rangle(1+\zeta(\langle\mu_z\rangle/\mu)^2)$, where $\xi = \Delta\nu_S/\Delta\nu$. Including an additional independent term describing the intrinsic LO–TO splitting, $\Delta\nu_B$, we obtain

$$\frac{\Delta\nu}{\nu_T} \approx \frac{\xi^{-1}E_S(\langle\mu_z\rangle/\mu)}{\langle E_{sym}\rangle\left[\left(1+\varsigma(\langle\mu_z\rangle/\mu)^2\right)\right]} + \frac{\Delta\nu_B}{\nu_T} \qquad (4)$$

Combining eqn (1) and (2) and using $\coth(x) \sim 1/x + 1/3\,x$, it may be shown that

$$\frac{\langle\mu_z\rangle}{\mu} = \frac{3T - 2\sqrt{\mu^2\zeta\langle E_{sym}\rangle(E_S - \langle E_{sym}\rangle) + 9T^2}}{2\mu\zeta\langle E_{sym}\rangle} \qquad (5)$$

From which it follows, using eqn (4) and $\Delta\nu = \Delta\nu_S + \Delta\nu_B$, that

$$\Delta\nu_S = \frac{\mu\xi\nu_T E_S T\left\{E_S\left[3T + \left(4\pi\mu^2\zeta\langle E_{sym}\rangle(E_S - \langle E_{sym}\rangle) + 9T^2\right)^{1/2}\right] - 6\langle E_{sym}\rangle T\right\}}{2\langle E_{sym}\rangle(E_S{}^2\mu^2\zeta + 9T^2)}\nu_T \qquad (6)$$

Since $E_S = 4\pi(\langle\mu_z\rangle/\mu)\mu/\Omega$, we can therefore derive $(\langle\mu_z\rangle/\mu)$ from

$$\langle\mu_z\rangle/\mu = \Omega E_S/4\pi\mu \quad (7)$$

We now set $\zeta = 43.8$, the value associated with $N_2O$, choosing this value since both the layer spacing and the dipole moment of $N_2O$ and CO in the solid state are closely similar. In this connection, $\Delta\nu_S$ evaluated through eqn (6), is insensitive at the $<5\%$ level to any relevant range of values of $\zeta$, between tens to $>10^4$.

We now proceed as in ref. 9, summarised as follows. With the help of eqn (4) to (7) we estimate $\langle E_{sym}\rangle$ from three pairs of simultaneous equations, each pair for two temperatures, use the resulting value of $\langle E_{sym}\rangle$ to obtain a value of $\Omega$ for a specific temperature, and use this to obtain $E_S$ and an estimate of $\langle\mu_z\rangle/\mu$. This sequence is performed for each of CSW, p-ASW and c-ASW for both $\Delta\nu_B = 2.119$ cm$^{-1}$ and 2.59 cm$^{-1}$. Results are shown in Table 5. Values of $E_S$ and $\langle\mu_z\rangle/\mu$ may be seen to be insensitive to the choice of $\Delta\nu_B$, as noted earlier.

As in ref. 9, the procedure outlined above did not yield a unique value of $\Omega$. For each case of CO-$p_{ASW}$, CO-$c_{ASW}$ and CO-CSW, two groups of values were encountered. One group consisted of low average values of 20, 14 and 39 $a_0^3$ for CO-CSW, CO-$p_{ASW}$ and CO-$c_{ASW}$ respectively and another group of high values, 172, 235 and 83 $a_0^3$. A recent paper[32] reported the correlation between polarizability, $\alpha$, and molecular volume and suggested the empirical relationship $\alpha = 0.0086\Omega^{4/3}$. Using $\alpha = 13.159$ au, we find $\Omega_{CO} = 244 \pm 30$ au. Evidently this would favour the group of higher values of $\Omega$, which we have used in preparing Table 5. For comparison, the value of $\Omega$ for CO–$SiO_2$ was found to be 273 au in ref. 9.

Solutions of eqn (6) for the spontelectric field yield two values for each deposition temperature and each ice substrate, with corresponding values of the degree of dipole orientation. For example CO-$p_{ASW}$ at 20 K has a field of both $3.73 \times 10^7$ V m$^{-1}$ and $8.79 \times 10^6$ V m$^{-1}$, referred to as the upper and lower branches respectively, representing a bi-metastable system as discussed briefly in ref. 9. In order to attempt to choose between these two sets values, we have recourse to values of the vibrational Stark shift of CO in the gas phase.[33] Following these values, average fields presented in Table 5, for the upper branch, would create a typical Stark shift of 0.71, 0.91 and 0.49 cm$^{-1}$ respectively for CO-CSW, CO-$p_{ASW}$ and CO-$c_{ASW}$. Values associated with the lower branch of the spontelectric field would be 0.17, 0.2 and 0.12 cm$^{-1}$. Observed Stark shifts are 0.89, 0.98 and 1.02 cm$^{-1}$ respectively, using the average values of $\Delta\nu_S/2$ with $\Delta\nu_B = 2.59$ cm$^{-1}$. Thus values for CO-CSW and CO-$p_{ASW}$ favour the adoption of the upper branch values of the spontelectric field, while values for CO-$c_{ASW}$ may leave some doubt. We will use values of the upper branch for all three cases in the remainder of this paper.

# 4. Discussion of results

## 4.1. Comparison with CO films on $SiO_2$

Results in Table 5 show three distinct regimes within the uncertainties associated with the data. First, CO deposited on $p_{ASW}$ has an essentially indistinguishable spontelectric field from CO–$SiO_2$. The corresponding degree of dipole orientation at 20 K is $0.0506 \pm 0.004$, taking the average of values in Table 5. This figure is $\sim$20% lower than for CO-$SiO_2$. Eqn (7) implies a correspondingly smaller value of $\Omega$, and we find a value $\sim$15% lower. Second, CO-$c_{ASW}$, by contrast with CO-$p_{ASW}$, shows a markedly weaker field than CO–$SiO_2$ films. Third, the spontelectric field for CO-CSW lies between CO-$p_{ASW}$ and CO-$c_{ASW}$. In addition, experimental errors in values of the spontelectric field obscure the detection of any trend of increase in the field with decreasing temperature of deposition.

The difference in the behaviour of CO-$c_{ASW}$, CO-CSW and CO-$p_{ASW}$ may most simply be attributed to a different structure of the CO film in each case. The only parameter in the model, which can be directly related to the aspect of structure, is the value of the effective molecular volume. Values lie in the approximate ratio 1 : 2 : 2.8 for CO-$c_{ASW}$, CO-CSW and CO-$p_{ASW}$. This may be related to different porosities in each case, where the underlying water structure templates the CO. This suggestion is supported by data for inhomogeneous broadening shown in Fig. 3, Section 2.2. Another speculative explanation may lie in the postulate that differing dipoles, created at the ice–CO interface, may influence the magnitude of an effective field in the overlying layer of CO.[11] In this case, the measured Stark effects would arise from a superposition of the spontelectric field and a spatially decaying field which arises from the interfacial dipole. The latter field would most likely be different for each type of underlying ice layer. Note that the presence of such a decaying non-spontelectric field is omitted from our analysis.

## 4.2. Relevance of spontelectric grains to astrophysical processes in regions of future star and planet formation: prestellar cores

There exist many examples in the Milky Way of dense condensations of gas, so-called prestellar cores, of dimension of a few tenths of a parsec (1 pc $\sim 3 \times 10^{16}$ m), where 'dense' implies local pressures of around $10^{-13}$ mbar. A number of observations show that the degree of ionization in these cores may be a factor of five to ten lower than elsewhere in the UV-shielded part of the interstellar medium (ISM),[15,16] given that the standard cosmic ray induced ionization fraction should be $\sim 3 \times 10^{-8}$ for a core of density $\sim 10^5$ cm$^{-3}$.[34–36] This has important consequences for the early stages of star formation, for example (i) *via* the chemistry and associated cooling rate, where heat is generated through gravitational contraction and requires to be lost to allow gravitational collapse, and (ii) through the weakness of measured magnetic fields encountered in these regions (see Section 4.2.3). We show below that the presence of polarization charging on the surface of grains, as our experimental data suggest, may lead to an understanding of the low level of ionization, from which springs so many properties related to star formation.

It is well-known from observation that CO is strongly depleted from the gas phase by freezing out onto interstellar grains in pre-stellar cores, as described for example in ref. 37. The layer of CO so formed would be almost pure or diluted

 

somewhat in $N_2$, to an unknown extent. We choose here to ignore this possible dilution, noting that dilution of the spontelectric material $N_2O$ in Xe, in equal quantities, reduces the spontelectric field by only $\sim$35%.[7] We recognize also that some CO may be converted to $CO_2$.[38] According to the experimental results presented here, grains in sufficiently cold regions, at $\leq$26 K, will therefore possess a polarization surface charge through the spontelectric effect. The remit in this section is limited to setting out some of the microscopic physics which arises from the possible presence of spontelectric CO ices on grains. In Section 4.2.1, we consider the rate of accumulation of CO ice mantles on grains and show that essentially all CO in the gas phase should be absorbed onto dust grains, as indeed can be observed. In Section 4.2.2 we estimate the rates of electrons and ions colliding with grains, using theory set out in ref. 39 as a guide. In Section 4.2.3 we outline the effect that spontelectric grains will have on the degree of ionization of the interstellar gas.

Pre-stellar cores are masses of weakly ionized plasma on the verge of gravitational collapse to form protostars. We use typical physical conditions which may be obtained, directly or indirectly, from observations of these cores. Such objects are found in a variety of environments, some of which may be rather isolated from any obvious external activity, such as the Bok globule B68 (*e.g.* ref. 40 and references therein), or others which may be closely associated with shocks from recently formed massive stars, such as in Orion.[41] Since B68 is the most intensively studied, we use physical conditions found there as a guide. These are as follows: number density of $H_2$, $n_{H_2}$ = $10^5$ cm$^{-3}$, [CO]/$H_2$ = $10^{-4}$ and kinetic temperature, $T$ = 10 K. We note that pre-stellar cores can possess a range of conditions; see Section 4.2.3. Observational data,[40,42,43] with data for the grain density, taken here to be 2 g cm$^{-3}$, and the proportion of the mass of the ambient medium contained in grains (0.013),[44] may be used to evaluate how many ML of CO may be found on a 'typical grain'. This may be shown to be $\sim$12 $(a_b/0.1)^{3/2}$ ML taking account of a small increase of grain radius as adsorption progresses (see Section 4.2.1). Here $a_b$ = grain radius in μm where this value is generally taken to be 0.1 μm.[45] Following recent data,[46] the thickness of $H_2O$ ice on grains should be limited to $\sim$30 ML as a maximum, increasing the effective grain radius by $\sim$10%, which we choose to ignore at this stage. The regions considered are sufficiently dense that UV radiation is excluded from the gas and grain charging is controlled by collisions with electrons and ions.

Water ice spectra, from observations of the ISM, show that generally the ice is in the form of compact amorphous ice,[47] referred to as $c_{ASW}$ above. In the subsequent analysis we therefore assume that $\phi$, the number of volts added per ML of CO = 6.695 $\times$ $10^{-3}$ V ML$^{-1}$, using the value for 21 K. In this connection, it is possible that the $p_{ASW}$ substrate in our experiments itself harboured a surface potential.[48] All symbols used in the forthcoming sections are defined in Table 6.

**4.2.1 Accretion of CO ice mantles.** As mentioned above, CO is strongly depleted in the denser part of pre-stellar cores, for example in B68[37] or in L1689B.[49] Therefore it might be sufficient simply to state that for $a_b$ = 0.1 μm, dust grains are covered by 10 to 15 ML (see above) and leave it at that. However it is our purpose here to compare timescales of CO accretion and ion and electron collisions with the grain in order to gain physical insight into the nature of spontelectric grain charging. We therefore seek first to show that almost all the available gas phase CO can condense on grains well within the lifetime of a pre-stellar core, which has been variously estimated but may be typically $\sim$4.5 $\times$ $10^5$ years.[50,51] The time of depletion has been estimated in earlier work (*e.g.* ref. 52) but the analysis was incomplete since the process was treated as exponential in time, treating the grain radius as independent of the quantity of CO adsorbed.

Table 6 Symbols used in Section 4. Standard values are shown in brackets

| Symbol | Description |
|---|---|
| $\phi$ | Number of volts added per ML of CO ($6.695 \times 10^{-3}$ V ML$^{-1}$ for $c_{ASW}$) |
| $q$ | Charge on the grain surface = $q$ e coulombs |
| $a_b$ | Grain radius (0.1 μm) |
| $a$ | Grain radius including CO mantle |
| $n_{ML}$ | Number of ML of CO on grain |
| $\delta$ | Density of grain material (2 g cm$^{-3}$) |
| $\xi$ | Grain-to-gas mass ratio (0.013) |
| $n_g$ | Number of grains per unit volume |
| $m_H$, $m_{CO}$ | Mass of H atom, CO molecule |
| $\alpha$ | Degree of ionization of the medium relative to $n_{H_2}$ ($3 \times 10^{-8}$, $5 \times 10^{-9}$) |
| $n_{H_2}$ | Number of $H_2$ molecules per unit volume ($10^{11}$ m$^{-3}$) |
| $T$ | Kinetic temperature (10 K) |
| $T_e$ | Electron temperature (10 K) |
| $s$ | Layer spacing (0.339 nm) |

The first order rate coefficient, $k^{1st}$, for removal of gas phase CO onto the grain surface is given by the velocity of CO times the cross-section presented by the grain. The number of grains per m$^3$ is given by 2.1 $n_{H_2} \cdot m_H \xi / \pi a^3 \delta$, with each presenting a cross-section for CO of $\pi a^2$, where a is the radius of the grain at time $t$. As time progresses, the radius of the grain will increase by $s n_{ML}$, where $n_{ML}$ is the number of monolayers and $s$ is the layer spacing (see Table 6). Hence

$$k^{1st} = (2.1\, n_{H_2} \cdot m_H \xi / \pi a^3 \delta) \cdot \pi a^2 \cdot (8kT/\pi m_{CO})^{1/2} = 6.26 \times 10^{-31}\, n_{H_2} T^{1/2}/a \quad (8)$$

where $a$ is a function of time. The rate of change of radius with time is given by $da/dt = s\, dn_{ML}/dt = 6.849 \times 10^{-19}$ s [CO] given that 1 ML requires $10^{19}$ CO molecules m$^{-2}$. Therefore the time to form one ML is $4 \times 10^{19}/\{(8kT/\pi m_{CO})^{1/2}[CO]\}$. This yields $n_{ML} = 6.849 \times 10^{-19}$ [CO]$t$. Thus the radius $a$, as a function of time follows $a = 6.849 \times 10^{-19}$ s [CO] $t + a_b$ where $a_b$ is the bare, or water ice covered, grain radius = $10^{-7}$ m.

Thus we obtain:

$$d[CO]/dt = -[CO]\,[(6.26 \times 10^{-31} n_{H_2}\, T^{1/2})/\{a_b + 6.849 \times 10^{-19}\,[CO]\, t\, s\}] \quad (9)$$

Inserting values of $T$ = 10 K, appropriate for B68, $a_b$ = $10^{-7}$ m and $s$ = 0.339 nm, we find the variation of [CO] with time shown

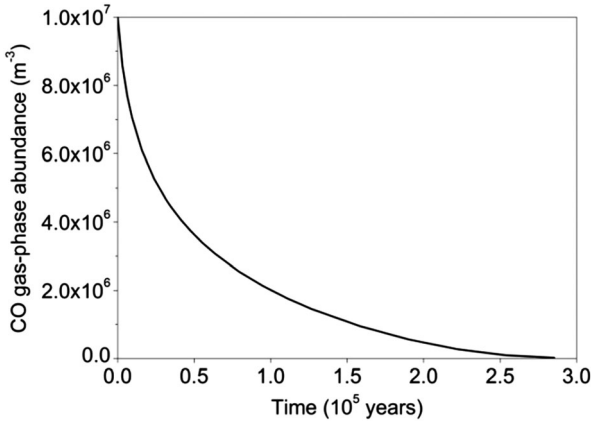


Fig. 4 The removal of CO with respect to time from the gas phase, initially at $10^7$ m$^{-3}$, through condensation onto dust grains, according to eqn (9). The physical conditions are CO/$H_2$ = $10^{-4}$, $n_{H_2}$ = $10^{11}$ m$^{-3}$, $T$ = 10 K, initial grain radius at $t$ = 0, $a_b$, = $10^{-7}$ m, with other relevant parameters given in Table 6.

in Fig. 4. In this figure it may be seen that effectively complete depletion (99.8% complete) takes place in $9 \times 10^{12}$ seconds = $2.85 \times 10^5$ years.

The time to form one ML is inversely proportional to CO, itself decreasing rapidly with time, and increases from an initial value of $1.8 \times 10^{11}$ seconds ($\sim$5700 years) to form 1 ML, rising to $1.2 \times 10^{12}$ seconds ($3.7 \times 10^4$ years) to form 5 ML and $4.0 \times 10^{12}$ seconds ($1.3 \times 10^5$ years) to form 10 ML. The corresponding growth of the CO film in terms of $n_{ML}$ *versus* time is shown in Fig. 5, where it may be seen that the film achieves $\sim$12 ML. The growth of the film will be accompanied by a growth in the positive polarization charge on the grain surface. This will be attended by an enhanced collision rate of electrons with the grain. We now address the question, in 4.2.2 below, of the relative timescales for CO condensation on the grain and the rate of electron collisions which tend to remove the spontelectric potential from the surface of the grain.

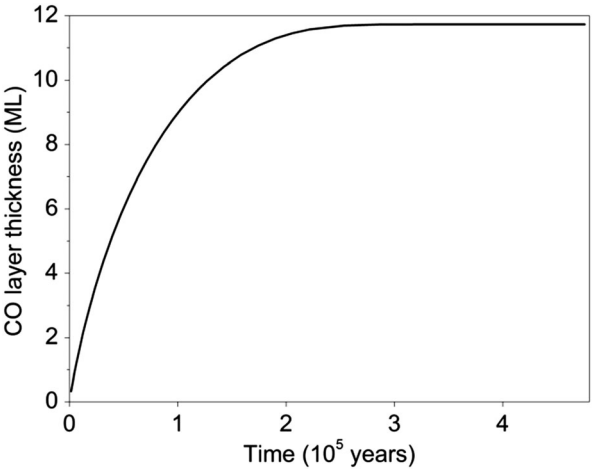


Fig. 5 The accumulation of monolayers of CO as a function of time on grains of initial radius 0.1 μm, for the physical conditions in B68 outlined in the text.

**4.2.2 Estimation of rates of electrons impacting on interstellar grains.** It is our purpose here to consider timescales for electron neutralization by gas phase electrons of the positive spontelectric polarization charge on CO mantles on grains. We find below that accumulation times for CO are very much greater than the time between collisions of electrons with grains. In a seminal paper of 1987, entitled 'Collisional Charging of interstellar Grains',[39] Draine and Sutin derived expressions for the rate of collisions of electrons with grains, for grains which are negatively charged, neutral and positively charged. These expressions involve essentially a cross-section times a velocity, in the normal manner, but multiplied by a factor, $f(\nu,\tau)$ which takes account of enhancement or reduction due to the charge state of the grain. $\nu$ is a signed quantity equal to the charge on the grain divided by the charge of the incident particle, here an electron or an ion, and $\tau$ is a reduced temperature defined in ref. 39. Account is taken, in estimating $f(\nu,\tau)$, of the electrostatic polarization of the grain by the approaching electron and the associated image potential. We treat the electrons as free particles and in this work ignore the possibility that any significant fraction is permanently attached to polycyclic aromatic hydrocarbons (PAHs).[53]

The conventional part of the rate coefficient in ref. 39 is given by the electron velocity in the plasma multiplied by the cross-sectional area of the grain. The first issue is therefore to determine the electron velocity. Electrons are formed at typically 20 eV by cosmic ray ionization of $H_2$ in shielded regions, as here. Electron energy is reduced rapidly to $\sim$10 eV through electronically inelastic collisions and, below this energy, electrons are cooled very largely by elastic collisions with $H_2$, with a cross-section[54,55] typically of $\sim$7.5 Å$^2$, which is approximately collision energy independent. Using our standard figure of $n_{H_2}$ = $10^{11}$ m$^{-3}$ and that each elastic collision removes $\sim$0.05 meV from the electron energy, $\sim 9 \times 10^6$ seconds is required for removal of 10 eV and to equilibrate with the kinetic temperature. We therefore set the effective electron temperature at the ambient kinetic temperature, since that this cooling is fast compared with other relevant processes, such as the accumulation of CO layers. We also note that the interstellar medium with $n_e$ = 500 m$^{-3}$ ($\alpha = 5 \times 10^{-9}$ – Table 6) and $T_e$ = 10 K, our standard conditions, has an associated Debye length of $\sim$10 m. Grains have a density of 0.73 m$^{-3}$ (see below) near the centre of B68, and thus the average distance apart of two such grains is $\sim$1.4 m. Notwithstanding, we will assume that the plasma remains quasi-neutral. Further, a simple estimate shows that electric fields due to electron and positive ion differential drift are negligible and therefore electrons and ions may be assumed to perform independent ballistic trajectories. Note also that, throughout, the influence of magnetic fields is ignored.

According to ref. 39, the rate of electron or ion collisions per second with grains is given by

$$J_e = n_e s_e (kT_e/m_e)^{1/2} \pi a^2 f(\nu,\tau)$$

or

$$J_i = n_i s_i (kT_i/m_i)^{1/2} \pi a^2 f(\nu,\tau) \quad (10)$$

 

where $f(\nu,\tau) = [1 + (4\tau + 3\nu)^{-1/2}]^2 \exp(-\theta_\nu/\tau)$ (attractive), $1 + (\pi/2\tau)^{1/2}$ (attractive), $(1 - (\nu/\tau))(1 + (2/(\tau - 2\nu))^{1/2})$ (repulsive) for negatively charged, neutral and positively charged grains and where $\theta_\nu = \nu/(1 + \nu^{-1/2})$. Here, $\nu$ is a positive or negative number, as appropriate, whose absolute value equals that of the effective charge on the grain, and $s_e$ and $s_i$ are the sticking coefficient for electrons and ions on grains.

For our case of a neutral plasma, with $a_b = 0.1$ μm and $n_{H_2} = 10^5$ cm$^{-3}$, we take the prevalent ion[44] to be $H^+$, that is, reduced mass $\mu_{H^+} = 1$, noting that this might require modification according to models presented in ref. 56. From this choice of the prevalent ion, it follows that $s_i^2 = s_e^2 = \mu_{H^+} = 1$, that is, 100% sticking efficiency may be assumed for both ions and electrons.[57,58] The principle to which we adhere is that the flux of electrons and positive ions to the grain must be equal on a time average and we find that we should set $\tau = 0.1$ to 0.2 in order that this may approximately hold. This implies a charge on the grain of $1/[1 + (\tau_0/\tau)^{1/2}] \sim -0.91$ where $\tau_0 = 1.39 \times 10^{-3}$.[39] Thus the average grain charge is negative, to repel the faster electrons and to attract the slower ions, as for any insulator immersed in neutral plasma. Throughout, we ignore any possible contribution from metal ions,[59] such as $Na^+$.

Using eqn (10), the timescales of encounters of relevance may be estimated. These estimates will be used in Section 4.2.3 for an assessment of the effect of spontelectric grains in the medium. Table 7 shows timescales for encounters of interest. The values of grain charge represent an initial value estimated above of −0.91, neutral grains and the value obtained by removal of an electron, that is, +1.09. An important conclusion is that all characteristic times are very short compared with the time to form 1 ML, say, of CO, which we estimated in Section 4.2.1 was typically $> 2 \times 10^{11}$ seconds.

**4.2.3 An assessment of the effects of spontelectric grains.** We consider here only one set of conditions, relevant to B68, namely $n_{H_2} = 10^5$ cm$^{-3}$, degree of ionization = $5 \times 10^{-9}$, $T = T_e = T_i = 10$ K, to investigate the outcome of the presence of spontelectric grains. We note that a variety of physical conditions may however be found in the literature for pre-stellar cores. For example $n_{H_2}$ in pre-stellar cores vary between a few $\times 10^4$ cm$^{-3}$ to $> 10^6$ cm$^{-3}$. The abundance of CO lies between $2.4 \times 10^{-5}$ in the core edge of L183[12] to the value of $8.5 \times 10^{-5}$ suggested for L1498 and L1517B13. The degree of ionization may be as low as $2 \times 10^{-9}$ in L1544[60] but may be more than an order of magnitude higher in other regions.

We first show that the proportion of electrons removed directly from the gas phase to the surface of grains, due to their spontelectric nature, is small, for the conditions of B68. We use as a basis for our estimate the result gleaned from Section 4.2.2 that the problem may be treated as an essentially static effect in which the accumulation of CO is offset instantaneously by the arrival of electrons, as shown in Section 4.2.2. The charge, $q$, on a grain of radius $a$ with $n_{ML}$ monolayers of CO is given by $4\pi\varepsilon_0 a n_{ML}\phi$. Given that $n_{ML} = 12$ (Section 4.2.1), the number of electrons attracted to each grain would be ∼5.75. The number of grains, $n_g$ per m$^{-3}$, is given by mass of the grains, equal to density of the grain material, $\delta$, times a grain volume, $4/3\pi a^3$, divided by the mass of gas, taking into account He, using a mass ratio of $\xi = 0.013$.[44,61] Thus $n_g$ is given by 2.1 $n_{H_2} \cdot m_H \xi/(\pi a_b{}^3 \delta)$ per m$^3$ = 0.73 m$^{-3}$. Therefore $0.73 \times 5.75 = 4.2$ electrons are removed per m$^3$, about 1% of the total given a value of $5 \times 10^{-9}$ $n_{H_2}$ for the total ionization of the medium. Note that here we ignore the variation with the grain radius as CO accumulates, since only rough estimates are made. The assumption is implicit that each polarization charge on the grain has unit efficiency in removing an electron from the gas phase. We conclude that the ∼12 ML layer of spontelectric CO (see Fig. 5) has a resulting polarization sufficient to remove only ∼1% of the electrons directly.

We consider a simple scenario which may govern the interaction of electrons with spontelectric grains. Initially, before any net adsorption of CO, values in Table 7, lines 1 and 4, show that an electron or ion will encounter the grain on the timescale of between 1 and $2 \times 10^7$ seconds. The spontelectric effect, being a macroscopic non-local phenomenon, requires a certain film thickness to develop. We know from ref. 9, that the effect is already active at 5 ML. Let us assume therefore that the spontelectric effect switches on at 5 ML, noting that the forthcoming argument does not turn upon this value. At this layer thickness, achieved after $1.18 \times 10^{12}$ seconds (see Fig. 5), the CO-grain surface will then abruptly tend to a state with a surface voltage of ∼33 mV. This is equivalent to ∼2.3 charges on average. Note that here and subsequently we assume that the value of $\phi = 6.695 \times 10^{-3}$ V ML$^{-1}$ is roughly independent of temperature, see Table 5, and use the same value at 10 K as measured at 21 K. Thus the grain surface, initially 0.91 negative, will become abruptly 1.4 positive, that is, some grains will possess one positive charge and some two. The latter figure of two positive charges would decrease the characteristic time for electron-grain encounters to $\sim 2 \times 10^5$ seconds from the value of $\sim 3 \times 10^5$ seconds for a single positive charge (see Table 7). The grain surface then proceeds *via* electron collisions through a neutral state, requiring a further $10^6$ seconds (Table 7), and subsequently both ions and electrons will again encounter the grain on the 1 to $2 \times 10^7$ seconds timescale.

Now, however, a new mechanism intervenes in which ions and mobile electrons recombine on the grain surface. This has long since been proposed as an important catalytic mechanism for the removal of charge from the gas phase.[57] If electrons are mobile on the grains, as we describe below, they will encounter and react with ions, creating neutrals. The electrons will initially be attracted, as the spontelectric effect becomes active, on the timescale of $3 \times 10^5$ seconds to the now positively

Table 7 Approximate timescales for encounters of charged particles with grains computed using $\tau = 0.2$ (see text) in eqn (10). $T_e = T_i = 10$ K, grain radius = 0.1 μm

| Projectile | Grain charge | Lifetime to encounter/s |
|---|---|---|
| e | −0.91 | 1 to $2 \times 10^7$ |
| e | Neutral | $10^6$ |
| e | 1.09 | $3 \times 10^5$ |
| $H^+$ | −0.91 | 1 to $2 \times 10^7$ |
| $H^+$ | Neutral | $4 \times 10^7$ |
| $H^+$ | 1.09 | 1 to $2 \times 10^9$ |

polarization-charged grain. Ions will follow on the 1 to $2 \times 10^7$ second timescale and the cycle will be continuously repeated as the CO layer builds up. As these processes proceed, the grains will little by little accumulate an average positive polarization charge of 5.75, at 12 ML, which will be offset by electrons from the gas phase and accompanied by the same number of positive ions. Thus after $\sim 8 \times 10^{12}$ seconds have elapsed, the time required to give effectively complete CO adsorption (Fig. 4), a state will be achieved with some well-defined average conditions, namely that in this state, each grain carries 5.75 electrons and an equal number of positive ions.

We now suggest that electrons and ions on the surface of the grain are continuously removed by recombination and continuously replenished from the gas phase, over a period of a further $6 \times 10^{12}$ seconds, where this time is taken from Fig. 5. Surface recombination was discussed in detail in ref. 57 and again in ref. 39, in which major corrections to the earlier publication were introduced. First however we discuss a phenomenological model and compare our results with those of ref. 39 below. Surface recombination requires mobile electrons on the grain surface, a topic discussed in detail in ref. 62. It was shown there that an electron has a residence time at any absorption site of $\sim 10^5$ seconds, for a grain temperature of 10 K, whereupon it may tunnel typically $\sim 20$ nm to a new site. If we regard the tunnelling length as defining the diameter of an area swept out by an electron in any one tunnelling event, then an electron will effectively cover the entire grain surface in $\sim 100$ residence times, that is, $\sim 10^7$ seconds and recombine with a static ion in $\leq 10^7$ seconds. Thus in the absence of the spontelectric effect, with only 0.91 ion and 0.91 electron together on any one grain on average, recombination may therefore take place on a timescale of $\leq 10^7$ seconds. The rate of recombination of ions, i, and electrons, e, on the grain surface, per grain, will be proportional to $[e_g]$ $[i_g]$, where these represent numbers per grain. The increase in efficiency of recombination due to the spontelectric effect will therefore be $(5.75/0.91)^2 \sim 40$, relative to the recombination efficiency associated with non-spontelectric grains, reducing the time for recombination to $\leq 2.5 \times 10^5$ seconds. A factor of $40^{1/2}$, that is, 6.3 increase in efficiency, compared with non-spontelectric grains, will be passed on directly to reduce the degree of ionization of the medium. This may be seen as follows.

The degree of ionization in the gas phase is determined through a steady state balance between the rate of cosmic ray ionization per volume per second, $\zeta_c\, n_{H_2}$, where $\zeta_c$ is typically $\sim 3 \times 10^{-17}$ s$^{-1}$ (see for example ref. 44), and all loss processes through ion-electron recombination, both in the gas phase and at the grain surface. In the gas phase, recombination processes are very largely determined by $e^- + H_3^+$. Here $H_3^+$ makes up $\sim 0.2$ of the total ionization[44] and the rate coefficient for recombination[63] is $\sim 2 \times 10^{-7}$ cm$^3$ s$^{-1}$ giving an effective coefficient, $k^{2nd}$, of $4 \times 10^{-8}$ cm$^3$ s$^{-1}$. If we balance this figure with $\zeta_c n_{H_2}$, we obtain [e] = [ions] = $(\zeta_c\, n_{H_2}/k^{2nd})^{1/2} \sim 8.7 \times 10^{-3}$ cm$^{-3}$, yielding an ionization fraction of $8.7 \times 10^{-8}$, whereas our standard observed value in B68 is $5 \times 10^{-9}$. Thus gas phase removal rate, $k^{2nd}$[e][ions], is too small to account for the low ionization in the medium.

We now compare this scenario with recombination on the grain surface. If the rate of loss of ionization on the surface of a single grain is given by $\kappa$ s$^{-1}$, then the rate of loss = $\kappa n_g$ cm$^{-3}$ s$^{-1}$ = $7.26 \times 10^{-12}$ $n_{H_2}\kappa$, given the relationship between the number of grains per unit volume and the hydrogen number density (see above), where $n_{H_2}$ here is expressed per cm$^3$. If we balance this with $\zeta_c n_{H_2}$, ignoring gas phase recombination, then we require $\kappa = 4.17 \times 10^{-6}$ s$^{-1}$ or $2.4 \times 10^5$ seconds between recombinations. This is essentially the time that was estimated above as the interval between electron–ion encounters on a grain surface ($\leq 2.5 \times 10^5$ seconds), given on average 5.75 electrons and ions present. Thus a model based on the presence of spontelectric grains in the medium gives essentially the same result as that which satisfies $\zeta_c n_{H_2}$ = rate of destruction of charge, where the latter gives the observed degree of ionization. This demonstrates that the presence of spontelectric grains can indeed reproduce the unexpectedly low degrees of ionization in B68 and by implication in other prestellar cores.

If only 0.91 ions and electrons are present on average, that is, in the non-spontelectric case, we have seen above that $\kappa$ is $\sim 40$ times smaller. Therefore in this case, the grain mechanism correspondingly fails by a factor of 6.3 to account for the degree of ionization observed. Thus we would suggest that the rate of removal of ions and electrons from the medium would, even under the circumstance of non-spontelectric grains, be governed by a dominant grain surface mechanism and a less effective gas phase mechanism. Taken together with the effect of the gas phase mechanism, which is $\sim 7.5$ less effective than the non-spontelectric grain surface mechanism, this yields a degree of ionization of $\sim 3 \times 10^{-8}$, a figure not atypical for the degree of ionization in regions obscured from UV light.[44,64]

We now consider values of surface recombination rate coefficients based upon the theoretical models in ref. 39, for comparison with the above estimates. We choose the model presented in ref. 39 rather than that in ref. 57, since this, as noted above,[39] includes the very significant contribution of the polarization interaction between the grain and ions or electrons. The relevant equation is 5.15 of ref. 39, which we note is sensitive to the choice of minimum grain size, to the power of $-1.5$, and also incorporates a significant contribution from very small grains, which may not be appropriate here.[65] At all events, in the present case we use the minimum radius of a grain as $10^{-8}$ m, the value quoted in ref. 39 as appropriate to the standard 'MRN' power law size distribution for grains.[66] Introducing the relevant values of kinetic temperature (10 K) and ion mass ($H^+$) into equation 5.15 of ref. 39 and equating the loss rate at the surface of a (non-spontelectric) grain with the cosmic ray production rate of ions as above, we find that the degree of ionization becomes $\sim 2.8 \times 10^{-8}$, including the gas phase contribution. This figure is essentially the same as that of $3 \times 10^{-8}$ deduced from the phenomenological model set out above for the non-spontelectric grain surface recombination case plus gas phase recombination. This agreement gives weight to our simple model.

We conclude that the effect of spontelectric grains is to enhance the removal of gas phase electrons and ions and

 

thereby to reduce considerably the degree of ionization under the physical conditions associated with the pre-stellar core B68, in this case by a factor of $\sim$6. There are some significant uncertainties in this estimate, perhaps principally in the assumption that the grain population can be adequately represented by $a_b$ = 0.1 μm. There is in fact growing observational evidence that the grain size distribution needs to be modified in prestellar cores to include a greater population of larger grains.[67,68] Thus in order to give more credence to the order of magnitude analysis presented above, the effects described should be incorporated into sophisticated time-dependent chemical models of pre-stellar cores, incorporating the latest data on grain size distribution. This is a problem well worth addressing since, in connection with the low ionization fraction found in pre-stellar cores, many such regions support a considerably weaker magnetic field than would be predicted by the standard empirical relationship $B = bn_0^{1/2}$ μG, where $b$ = 1 to 5 and $n_0 = 2n_{H_2} + n_H$. For example, in the prestellar cores L1498 and L1517B, fields are 10 $\pm$ 7 and 30 $\pm$ 10 μG, respectively, whereas the derived densities are $10^5$ cm$^{-3}$ and 6 $\times$ $10^5$ cm$^{-3}$, suggesting fields of $>$300 or $>$800 $\mu$G. A reduction in ion and electron density through a sizeable factor, through the action of spontelectric grains, may contribute to the weakness of the magnetic field. This will be accompanied by a loss of magnetic pressure to withstand gravitational collapse. There are a number of other areas in which the reduction of the degree of ionization will affect star formation, for example the loss of angular momentum from the gas to the grains, and the release of CO from the grain on warming, as a protostar forms, and the possible accompanying re-establishment of a larger magnetic field.

## 5. Summary and concluding comments

The main thrust of this paper is the experimental work which verifies that solid CO on water ice is spontelectric and shows that the magnitude of the spontelectric field depends on the nature of the ice on which the material is laid down. We find that relative to CO on a $SiO_2$ substrate,[9] the strength of the spontelectric field is in the ratio 1 : 0.76 : 0.52 for CO-$p_{ASW}$, CO-CSW and CO-$c_{ASW}$ respectively, for a deposition temperature of 20 K for CO-$p_{ASW}$ and CO-CSW and 21 K for CO-$c_{ASW}$.

The choice of substrates was made with a view to astrophysical applications. The normal circumstance in molecular clouds is that grains possess on average a single negative charge, given that they are shielded from an ultraviolet field. If the temperature is $\lesssim$100 K, observations show that grains tend to be coated with $c_{ASW}$.[47] As the temperature falls below $\sim$26 K, we have shown that a total of 12 ML of spontelectric CO ice can form on this substrate on a time scale about half of that of the expected lifetime of the prestellar phase of star formation, under the conditions of $10^5$ $H_2$ cm$^{-3}$ and $T$ = 10 K, representative of the pre-stellar core B68. The net result of the CO ice is that grains become spontelectric, attracting electrons and positive ions to their surface, where these species undergo recombination. This reveals a spontelectric grain as essentially a catalyst for the removal of ionization from the gas phase. The spontelectric grain surface recombination mechanism takes over from the gas phase recombination of $e^- + H_3^+$, plus the non-spontelectric grain surface mechanism, as the dominant means of removing ions and electrons from the medium. Put succinctly, cosmic rays are the source for ionization and spontelectric grains now provide the major sink. This results in values of fractional ionization relative to $H_2$ of 5 $\times$ $10^{-9}$ in B68, compared with the more familiar value of 3 to 5 $\times$ $10^{-8}$ in molecular cloud cores.[69–71] In general the degree of ionization is reduced by a factor equal to the number of electrons (or ions) trapped in the steady state on the spontelectric grain surface, given some grain radius. Here we have used the standard value for the bare grain of $a_b$ = 0.1 μm, giving in B68 the number of trapped electrons or ions equals $\sim$6, where such a steady state value is established after $\sim$2.5 $\times$ $10^5$ years. The presence of spontelectric grains may indeed be the root of the low ionization fraction observed in prestellar cores in general, where these show strong CO depletion. This should however most properly be seen as a postulate rather than a proof, since it is possible that other general explanations for a contribution to low fractional ionizations may be forthcoming. A contributory factor may for example be a reduction of the cosmic ray ionization rates in dense regions, which according to ref. 72 fall by between 25% and 40% in the prestellar cores L1498 and L1517B.

## Acknowledgements

We gratefully acknowledge support of the staff of the Aarhus Synchrotron Radiation Laboratory (ISA), the Danish Research Council, European Community FP7-ITN Marie-Curie Programme (LASSIE project, grant agreement #238258; AC, JL), Heriot-Watt University for a James Watt scholarship (ARF) and the experimental assistance of Ms Holly Glenister.

## References

1 D. Field, O. Plekan, A. Cassidy, R. Balog, N. C. Jones and J. Dunger, *Int. Rev. Phys. Chem.*, 2013, **32**, 345–392.
2 R. Balog, P. Cicman, N. Jones and D. Field, *Phys. Rev. Lett.*, 2009, **102**, 2–5.
3 D. Field, O. Plekan, A. Cassidy, R. Balog and N. Jones, *Europhys. News*, 2011, **42**, 32–35.
4 O. Plekan, A. Cassidy, R. Balog, N. C. Jones and D. Field, *Phys. Chem. Chem. Phys.*, 2011, **13**, 21035–21044.
5 O. Plekan, A. Cassidy, R. Balog, N. C. Jones and D. Field, *Phys. Chem. Chem. Phys.*, 2012, **14**, 9972–9976.
6 A. Cassidy, O. Plekan, R. Balog, N. C. Jones and D. Field, *Phys. Chem. Chem. Phys.*, 2012, **15**, 108–113.
7 A. Cassidy, O. Plekan, J. Dunger, R. Balog, N. C. Jones, J. Lasne, A. Rosu-Finsen, M. R. S. McCoustra and D. Field, *Phys. Chem. Chem. Phys.*, 2014, **16**, 23843.

8 J. Lasne, A. Rosu-Finsen, A. Cassidy, M. R. S. McCoustra and D. Field, *Phys. Chem. Chem. Phys.*, 2015, **17**, 20971.
9 J. Lasne, A. Rosu-Finsen, A. Cassidy, M. R. S. McCoustra and D. Field, *Phys. Chem. Chem. Phys.*, 2015, **17**, 30177.
10 S. G. Boxer, *J. Phys. Chem. B*, 2009, **113**, 2972.
11 A. Cassidy, O. Plekan, R. Balog, J. Dunger and D. Field, *J. Phys. Chem.*, 2014, **118**, 6615.
12 L. Pagani, A. Bourgoin and F. Lique, *Astron. Astrophys.*, 2012, **548**, L4.
13 C. J. Lada, E. A. Bergin, J. F. Alves and T. L. Huard, *Astrophys. J.*, 2003, **86**, 286.
14 M. P. Collings, J. W. Dever and M. R. S. McCoustra, *Phys. Chem. Chem. Phys.*, 2014, **16**, 3479.
15 P. Caselli, C. M. Walmsley, A. Zucconi, M. Tafalla, L. Dore and P. C. Myers, *Astrophys. J.*, 2002, **565**, 344.
16 S. Maret and E. A. Bergin, *Astrophys. J.*, 2007, **664**, 956.
17 D. Berreman, *Phys. Rev.*, 1963, **130**, 2193.
18 L. H. Jones and B. I. Swanson, *J. Phys. Chem.*, 1991, **95**, 2701.
19 M. A. Ovchinnikov and C. A. Wight, *J. Chem. Phys.*, 1993, **99**, 3374.
20 M. A. Ovchinnikov and C. A. Wight, *J. Chem. Phys.*, 1994, **100**, 972.
21 H. J. Fraser, M. P. Collings and M. R. S. McCoustra, *Rev. Sci. Instrum.*, 2002, **73**, 2161.
22 V. L. Frankland, A. Rosu-Finsen, J. Lasne, M. P. Collings and M. R. S. McCoustra, *Rev. Sci. Instrum.*, 2015, **86**, 055103.
23 J.-B. Bossa, K. Isokoski, M. S. de Valois and H. Linnatrz, *Astron. Astrophys.*, 2012, **A82**, 545.
24 S. Townrow, P. G. Coleman, Y. C. Wu, J. Jiang and S. J. Wang, *J. Phys.: Conf. Ser.*, 2013, **443**, 012058.
25 M. J. Wojcik, V. Buch and J. P. Devlin, *J. Chem. Phys.*, 1993, **99**, 2332.
26 M. P. Collings, J. W. Dever, H. J. Fraser, M. R. S. McCoustra and D. A. Williams, *Astrophys. J.*, 2003, **583**, 1058.
27 M. P. Collings, J. W. Dever, H. J. Fraser and M. R. S. McCoustra, *Astron. Astrophys.*, 2003, **285**, 633.
28 M. P. Collings, V. L. Frankland, J. Lasne, D. Marchione, A. Rosu-Finsen and M. R. S. McCoustra, *Mon. Not. R. Astron. Soc.*, 2015, **449**, 1826.
29 V. F. Petrenko and R. W. Whitworth, *Physics of Ice*, Oxford University Press, 1996.
30 C. Kittel, *Introduction to Solid State Physics*, Wiley, 3rd edn, 2005.
31 J. Topping, *Proc. R. Soc. London, Ser. A*, 1927, **114**, 67.
32 S. A. Blair and A. J. Thakkar, *J. Chem. Phys.*, 2014, **141**, 074306.
33 S. S. Hashjin and C. F. Matta, *J. Chem. Phys.*, 2013, **139**, 144101.
34 B. G. Elmegreen, *Astrophys. J.*, 1979, **232**, 729.
35 T. Nakano, *Publ. Astron. Soc. Jpn.*, 1979, **31**, 697.
36 P. Padoan, K. Willacy, W. Langer and M. Juvela, *Astrophys. J.*, 2004, **614**, 203.
37 E. A. Bergin, J. Alves, T. Huard and C. J. Lada, *Astrophys. J., Lett.*, 2002, **570**, L101.
38 R. T. Garrod and T. Pauly, *Astrophys. J.*, 2011, **735**, 15.
39 B. T. Draine and B. Sutin, *Astrophys. J.*, 1987, **320**, 803.
40 M. Nielbock, R. Launhardt, J. Steinacker and A. M. Stutz, *Astron. Astrophys.*, 2012, **547**, L4.
41 H. D. Nissen, N. J. Cunningham, M. Gustafsson, J. Bally, J.-L. Lemaire, C. Favre and D. Field, *Astron. Astrophys.*, 2012, **540**, A119.
42 D. C. B. Whittet, P. F. Goldsmith and J. L. Pineda, *Astrophys. J.*, 2010, **720**, 259.
43 T. Güver and F. Özel, *Mon. Not. R. Astron. Soc.*, 2009, **400**, 2050.
44 C. M. Walmsley, D. R. Flower and G. Pineau des Forêts, *Astron. Astrophys.*, 2004, **418**, 1035–1043.
45 B. T. Draine, *Annu. Rev. Astron. Astrophys.*, 2003, **41**, 241.
46 C. A. Poteet, D. C. B. Whittet and B. T. Draine, *Astrophys. J.*, 2015, **801**, 110.
47 E. F. van Dishoeck, E. Herbst and D. A. Neufeld, *Chem. Rev.*, 2013, **113**, 9043.
48 C. Bu, J. Shi, U. Raut, E. H. Mitchell and R. A. Baragiola, *J. Chem. Phys.*, 2015, **142**, 134702.
49 M. P. Redman, J. M. C. Rawlings, D. J. Nutter, D. Ward-Thompson and D. A. Willams, *Mon. Not. R. Astron. Soc.*, 2002, **337**, L17.
50 M. L. Enoch, N. J. Evans, A. I. Sargent, J. Glenn, E. Rosolowsky and P. Myers, *Astrophys. J.*, 2008, **684**, 1240.
51 J. L. Pineda, P. F. Goldsmith, N. Chapman, R. L. Snell, D. Li, L. Cambrésy and C. Brunt, *Astrophys. J.*, 2010, **721**, 686.
52 E. A. Bergin and M. Tafalla, *Annu. Rev. Astron. Astrophys.*, 2007, **45**, 339.
53 F. Carelli, T. Grassi and F. A. Gianturcox, *Astron. Astrophys.*, 2013, **549**, A103.
54 M. A. Khakoo and S. Trajmar, *Phys. Rev. A: At., Mol., Opt. Phys.*, 1986, **34**, 138.
55 J. Randell, S. L. Lunt, G. Mrotzek, J.-P. Ziesel and D. Field, *J. Phys. B: At., Mol. Opt. Phys.*, 1994, **27**, 2369.
56 K. Tassis, K. Willacy, H. W. Yorke and N. J. Turner, *Astrophys. J.*, 2012, **754**, 6.
57 T. Umebayashi and T. Nakano, *Publ. Astron. Soc. Jpn.*, 1980, **32**, 405.
58 E. Dartois and L. d'Hendecourt, *Astron. Astrophys.*, 1997, **323**, 534.
59 M. Oppenheimer and A. Dalgarno, *Astrophys. J.*, 1974, **192**, 29.
60 J. F. Alves, C. J. Lada and E. A. Lada, *Nature*, 2001a, **409**, 59.
61 B. Parise, A. Belloche, F. Du, R. Gusten and K. M. Menten, *Astron. Astrophys.*, 2011, **526**, A31.
62 D. Field, *Astron. Astrophys.*, 2000, **362**, 774.
63 P. Rubovic, P. Dohnal, M. Hejduk, R. Plasil and J. Glosik, *J. Phys. Chem. A*, 2013, **117**, 9626.
64 P. Caselli, C. M. Walmsley, R. Tervieza and E. Herbst, *Astrophys. J.*, 1998, **499**, 234.
65 D. Stamatellos, A. P. Whitworth and D. Ward-Thompson, *Mon. Not. R. Astron. Soc.*, 2007, **379**, 1390.
66 J. S. Mathis, W. Rumpl and K. H. Nordsieck, *Astrophys. J.*, 1997, **217**, 425.
67 J. Steinacker, C. W. Ormel, M. Andersen and A. Bacmann, *Astron. Astrophys.*, 2014, **564**, A96.

 

68 J. Steinacker, M. Andersen, W.-F. Thi, R. Paladini, M. Juvela, A. Bacmann, V.-M. Pelkonen, L. Pagani, C. Lefèvre, T. Henning and A. Noriega-Crespo, 2015, http://arxiv.org/pdf/1508.04691.pdf.
69 M. Guelin, W. D. Langer, R. L. Snell and H. A. Wootten, *Astrophys. J.*, 1977, **217**, L165.
70 W. D. Langer, R. W. Wilson, P. S. Henry and M. Guelin, *Astrophys. J.*, 1978, **225**, L139.
71 W. D. Watson, L. E. Snyder and J. M. Hollis, *Astrophys. J.*, 1978, **222**, L145.
72 M. Padovani, P. Henebelle and D. Galli, *Astron. Astrophys.*, 2013, **560**, A114.